Clean Technologies and Recycling

https://www.aimspress.com/journal/ctr

Clean Technologies and Recycling, 5 (1): 44–63.
DOI: 10.3934/ctr.2025003
Received: 04 November 2024
Revised: 07 April 2025
Accepted: 27 May 2025
Published: 05 June 2025

Research article

Quantification of moisture in household plastic packaging waste using near-infrared hyperspectral imaging (NIR-HSI)

Pim van den Brink[1], Stefan Bontekoe[1], Homer C. Genuino[1] and Marcel C. P. van Eijk[1,2,*]

[1] NTCP, Duitslanddreef 7, 8447 SE Heerenveen, the Netherlands
[2] Circular Chemical Engineering, Maastricht University, Urmonderbaan 22, 6167 RD Geleen, the Netherlands

* **Correspondence:** Email: mvaneijk@ntcp.nl; Tel: +31 6 5055 7408.

Abstract: Quantifying moisture in plastic waste is crucial for optimizing recycling processes and improving the quality of recycled materials. Conventional methods, such as gravimetric analysis, are laborious and energy-intensive, limiting their efficiency in high-throughput industrial environments. This study presents and validates the use of near-infrared hyperspectral imaging (NIR-HSI) as a rapid, non-destructive method for moisture analysis in household plastic packaging waste (i.e., PE and PP films and rigids, PET, mixed plastics). By utilizing an NIR-HSI camera on a data collection conveyor belt, samples with varying moisture levels were analyzed. The method employs univariate calibration, correlating NIR absorbance from water with moisture concentration determined by the standard gravimetric method. To ensure accuracy, NIR absorbance from water was isolated by identifying and eliminating polymer-related absorbance through peak annotation. Principal component analysis (PCA) was subsequently applied to distinguish between rigids and films. Further refinement was achieved by normalizing the spectra and subtracting a dry reference spectrum, effectively eliminating the polymer signal. This approach enabled accurate quantification of moisture content and provided spatially resolved information on moisture distribution, including subsurface moisture. The method was successfully implemented in a pilot-scale sorting facility, where 95% of measurements achieved an accuracy within 2.6 percentage points. This integration underscores the significant potential of NIR-HSI for inline analysis and real-time feedback in recycling operations, offering significant advancements for future research and industrial applications in plastic waste recycling.

Keywords: plastic recycling; moisture quantification; near-infrared hyperspectral imaging (NIR-HSI); principal component analysis (PCA); inline analysis

1. Introduction

Plastic waste management has become a pressing global challenge, especially due to its environmental impact [1]. The recycling process, from waste collection to the production of clean flakes suitable for reactor or extruder inputs, is hindered by significant gaps in quality data. These data deficiencies arise from the lack of appropriate methods to quantify the presence of various contaminants, in particular moisture and surface contamination, within recycling streams in industrial settings [2]. Previous studies reported that moisture levels in plastic waste can vary widely, from 5 wt% to approximately 30 wt%, depending on plastic type, environmental exposure, and handling processes [3,4]. Excessive moisture in plastic waste poses a threat to process efficiency and mass balance calculations. Moreover, moisture-laden plastics are often considered less desirable for recycling as they can negatively impact the quality of the recycled material, introduce additional handling and transportation costs, and promote degradation, leading to weakened and brittle plastics [5,6]. Furthermore, moisture can foster microbial growth, degrading both the appearance and structural integrity of plastics, which further reduces their recyclability [7].

In recycling processes, the effects of excessive moisture can vary depending on the technology used. For example, in chemical recycling processes such as pyrolysis, moisture in the feedstock leads to unwanted byproducts, reduced yield, and an altered composition of the pyrolysis oil, complicating downstream processes [8]. In mechanical recycling, moisture-laden or contaminated plastics often fail to meet the quality standards required for recycled products, diminishing their market value and usability [9]. Additionally, unaddressed moisture can facilitate leaching of contaminants from the plastic into the surrounding environment, posing additional environmental risks [10]. Removing excess moisture from plastic waste requires energy, whether through mechanical or thermal drying [11]. Therefore, accurate knowledge of the initial moisture content helps to estimate the required drying expenditure and optimize the overall energy consumption in recycling.

Traditional methods for moisture quantification in plastic waste, such as gravimetric analysis, involve drying representative samples to a constant weight in an oven at temperatures up to 95°C [12–15]. While effective, this process is labor-intensive, time-consuming, and not suitable for high-throughput industrial applications where large, heterogeneous samples are prevalent. Additionally, gravimetric methods lack the capacity for real-time analysis and often struggle with inconsistent moisture distribution across the waste stream, which can lead to inaccuracies in quantification. Although automated thermogravimetric analyzers offer continuous monitoring, their use in industrial settings remains limited due to plastic waste complexity.

In response to these challenges, alternative moisture quantification methods, including microwave moisture analysis, radio frequency sensing, and capacitance measurements, have been explored for inline monitoring. Microwave moisture analysis utilizes dielectric heating to assess moisture levels, while radio frequency sensing measures impedance or capacitance changes due to moisture [16–20]. Capacitance measurement techniques, which monitor dielectric property changes with moisture, are suited for integration in production lines for real-time readings. Infrared thermography, another non-contact method, rapidly measures surface temperatures to infer moisture content, making it suitable for inline applications [21]. These methods vary in terms of accuracy, sensitivity, and suitability for different plastics and conditions, and have yet to be fully adapted for plastic waste, highlighting the need for robust, non-destructive moisture quantification techniques for recycling applications.

The main challenge that hinders the applicability of the techniques outlined above is the heterogeneity of post-consumer plastic waste. In other fields, the calibration of the signal is based on a known material density or constant flow speed, both of which are not possible with plastic waste on an object level. A solution could be to determine the exact material flow after which variabilities can be accounted for; however, this is rather challenging.

Near-infrared (NIR) spectroscopy has proven effective for moisture quantification in diverse materials, from agricultural products to cellulosic materials like wood and paper [22–24]. Research on moisture measurements in agricultural products using NIR spectroscopy has documented errors ranging from 5% to 10%, attributed to factors such as sample heterogeneity and surface characteristics [22–24]. The sensitivity of NIR methods derives from the strong absorption of water in the NIR range, particularly at 1450 and 1940 nm, attributed to the O-H stretching and bending vibrations [25,26]. NIR hyperspectral imaging (NIR-HSI) integrates the capabilities of NIR spectroscopy and hyperspectral imaging, creating a powerful technique for real-time, non-destructive analysis of plastic samples on a conveyor belt [27]. In this technique, halogen lamps illuminate the sample, and an NIR sensor detects the reflected light, generating spatially resolved data. Each pixel in the dataset corresponds to a unique spectral signature, enabling detailed mapping of moisture distribution across and within the sample, thus providing a capability beyond traditional point-based NIR sensors [28–30].

NIR-HSI has shown potential for applications in plastic waste management, offering accurate, non-destructive moisture quantification that can improve quality control in recycling processes. NIR-HSI can differentiate plastics by their spectral signatures, aiding in the separation of moisture-laden or contaminated materials from recyclable ones. Real-time moisture monitoring during recycling allows for optimized process parameters and enhancing efficiency across the recycling chain—from collection and transit to material recovery facilities (MRFs) and finally, to recycling facilities. While existing NIR spectroscopic methods have limitations in industrial plastic waste moisture monitoring, NIR-HSI holds promise for overcoming these barriers due to its high spatial resolution and ability to generate detailed moisture maps.

Despite its potential, studies on moisture quantification in plastic waste using NIR-HSI remain limited. The current study seeks to address this gap by developing a reliable method for accurately quantifying moisture content in authentic plastic waste through NIR-HSI. Using a hyperspectral imaging setup, NIR-HSI images of plastic waste samples were captured on a conveyor belt, and the resulting data were processed to isolate and quantify NIR light absorbance associated with water content. This absorbance was subsequently correlated to moisture content determined via gravimetric methods, also offering validation and comparability. Furthermore, this study provides valuable data on moisture distribution within plastic materials, which can be critical for optimizing industrial drying and processing steps. Testing this method in a pilot-scale sorting facility using real household plastic packaging waste confirmed its reliability and demonstrated that NIR-HSI can overcome limitations of traditional approaches. Thus, this approach in moisture quantification has the potential to significantly improve the monitoring and management of plastic waste in industrial settings.

2. Materials and methods

2.1. Sample preparation

Plastic packaging waste, namely polyethylene (PE) and polypropylene (PP) films, PE and PP rigids, and polyethylene terephthalate (PET) were manually sorted from batches of DKR-350 mixed plastic waste stream [31] and DKR-310 [32] (approximately 50 kg per batch) supplied by PreZero Nederland B.V. (Zwolle, the Netherlands). DKR is a classification used in Europe, particularly within the German system, to describe a specific type of plastic waste predominantly collected from household packaging materials. PE, PP, and PET represent the most common types of plastics in household packaging waste. These materials come in the form of rigid packaging, such as bottles, trays, and cups, but also in the form of film packaging, such as bags and wrappings. For each sorted stream, a random selection of 50 objects was used to create a calibration sample. PET film was excluded due to the low quantity present in plastic packaging waste, as it is hardly used as primary packaging. The objects were washed and wet to various moisture levels, then analyzed using a hyperspectral camera. Samples were subsequently dried at 90–95°C for 6 h to calculate moisture content, using the formula

$$w_{\mathrm{water}} = \frac{m_0 - m_{\mathrm{d}}}{m_0}$$

where m_0 represents the initial mass, m_{d} the dried mass, and w_{water} the mass fraction of water. This approach linked hyperspectral data with moisture concentrations determined by the standard gravimetric method. Model validation was performed using an independent set of samples with known moisture levels. Unlike calibration samples, validation samples (ranging from 1 to 3 kg) were sorted from the DKR-350 stream and were not washed or subjected to controlled moisture addition. The accuracy and reliability of the model were evaluated by comparing predicted moisture values to actual values obtained by gravimetric analysis.

2.2. Data collection

Hyperspectral data were collected using a SPECIM FX 17 NIR-HSI camera (Specim, Oulu, Finland) mounted on a conveyor belt platform (Figure 1). The camera was equipped with an 8 mm focal length lens. To replicate real recycling conditions and reduce spectral distortions, a halogen lamp was positioned 36 cm above the conveyor belt to provide uniform lighting. An InGaAs detector array with a grating prism monochromator captured reflected wavelengths in the 900–1700 nm spectral range. The camera resolution consisted of 640 spatial pixels in width, with each pixel containing 224 discrete reflectance values, and image acquisition was acquired by Lumo recorder software.

As shown in Figure 2, each hyperspectral dataset forms a data cube by combining two spatial dimensions (x and y) with a spectral dimension (wavelength). Each pixel within the spatial domain (xy plane) provides a unique spectral signature, represented by a pixel vector, with intensity values spanning 224 wavelength bands. This integration of spatial and spectral data allows for detailed characterization of plastic materials.

Figure 1. Photographs of the actual data collection platform used, integrating Specim FX 17 camera and the halogen light source used for data collection (left); Actual plastic waste samples on the conveyor belt (right).

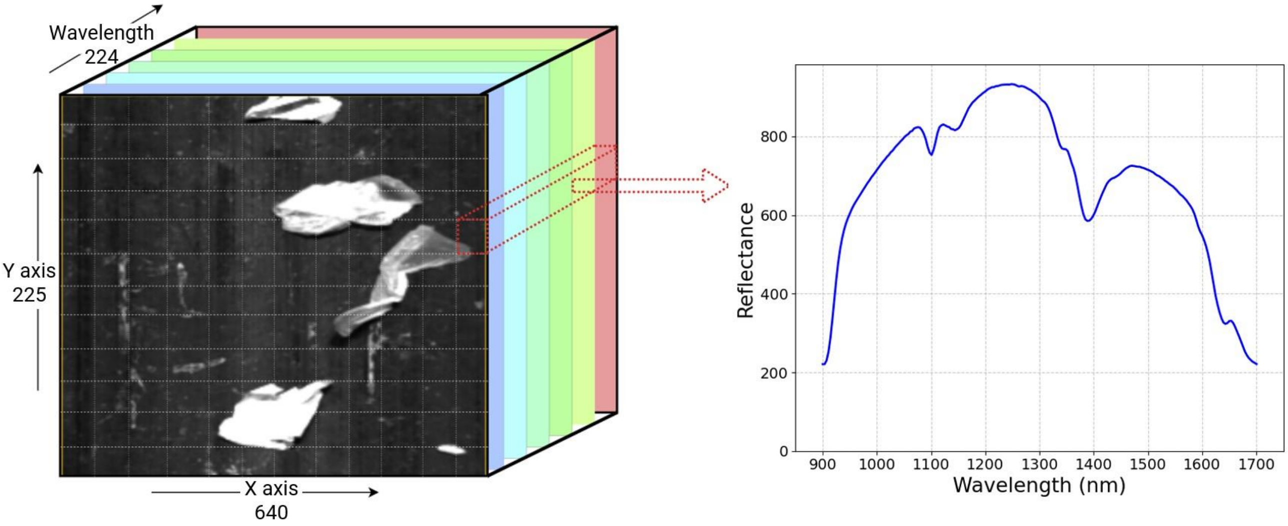

Figure 2. Hyperspectral data cube representation and spectral extraction for plastic waste analysis: 3D hyperspectral data cube with spatial dimensions, where each pixel in spatial domain contains a unique spectral signature across wavelengths (left). Example of a reflectance spectrum extracted from a pixel within the data cube (right).

For fast data processing, a program was developed to automate the analysis of all captured images. The spectrum of each pixel was identified (using the peak annotation flowchart shown in Figure 3) and saved according to the corresponding plastic type. Evidently, most black objects could not be identified due to the absorption of NIR light by the pigment. Some black pigments, other than carbon black, do allow for material recognition if their absorption spectrum is not located in the NIR region; those are, however, not used as frequently as carbon black. It should be noted that the use of carbon black in packaging is decreasing. Moreover, surface contamination could interfere with material recognition because of the limited penetration depth of the light. However, for some additives, given their typically low concentrations and spectral normalization techniques employed, their impacts were significantly mitigated. After all pixels were processed, averaged spectra for each material type were calculated and analyzed to determine moisture absorbance and concentration using univariate calibration.

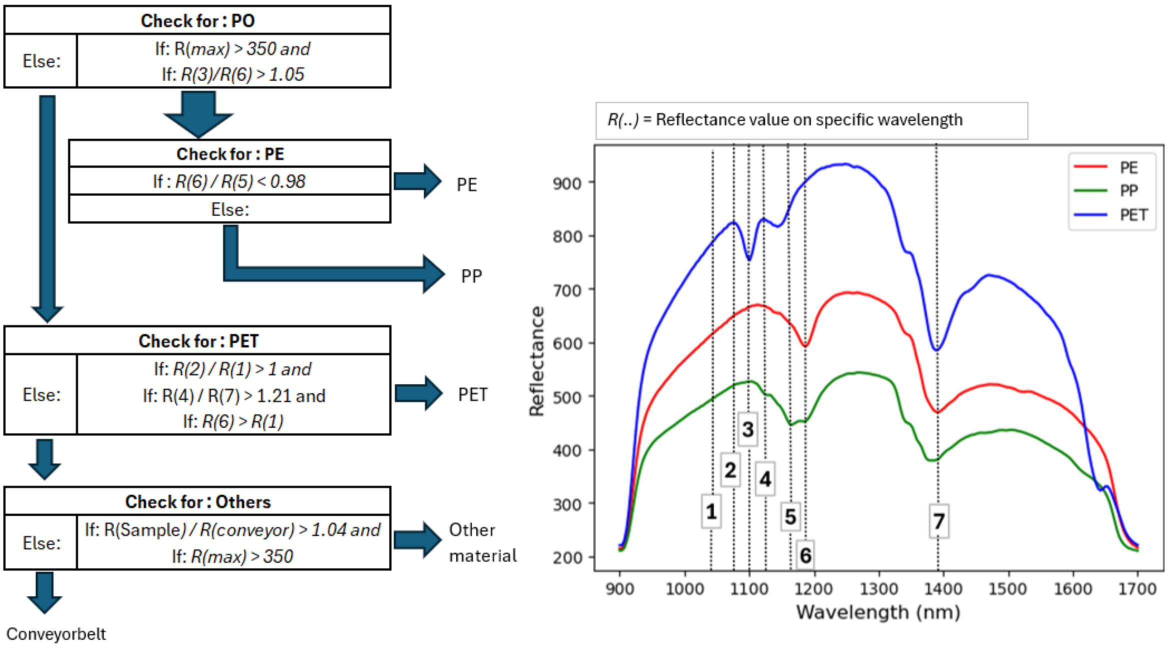

Figure 3. Classification flowchart and spectral characteristics of plastic types used in NIR-HSI analysis: stepwise decision tree applied to identify PE, PP, PET, and other materials based on reflectance (*R*) ratios at specific wavelengths (left). Representative *R* spectra for PE, PP, and PET, with key wavelengths highlighted to indicate points of spectral distinction.

2.3. Plastic characterization

Spectral data processing was performed to isolate moisture-specific absorbance from plastic polymer absorbance. Automated plastic type identification was achieved using a peak annotation model (Figure 3), which compared reflectance values (*R*) at different wavelengths to classify each pixel. Pixels identified as part of the conveyor belt were discarded, significantly reducing data volume and improving processing speed. Alternatively, full-spectrum processing, followed by pixel classification, can increase accuracy but also extend processing time. By mapping each classified pixel, an image of the spatial distribution of plastic types was generated (Figure 4). Different plastic types were color-coded, enhancing visualization of spatial heterogeneity (e.g., red for PE, green for PP, and blue for PET).

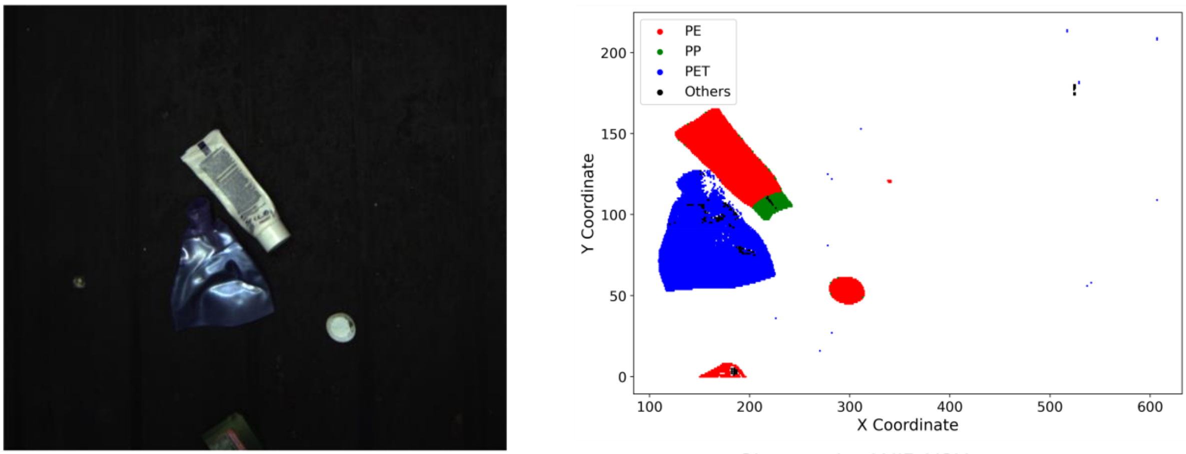

RGB

Characterized NIR-HSI image

Figure 4. Visualization of material classification map for plastic waste: RGB image of assorted plastic waste items (e.g., PE tube, PP cup, and PET bottle) (left). Same scene after processing with NIR-HSI for material characterization, with color coding.

2.4. Identification of rigids and films

The initial model described above could not reliably distinguish rigid plastics from films due to the limited sensitivity of the classification rules in Figure 3. Given the substantial differences in surface area, density, and water retention characteristics between rigids and films, it is crucial to differentiate between these forms. NIR spectra from rigid plastics differ from film plastics. These differences are mainly caused by the increased path length of NIR light in rigid plastics, enabling higher specific absorption. Since these effects are subtle and material heterogeneity introduces substantial noise, single spectra are not consistent enough to give reliable classification.

To improve accuracy, spatial data clustering was applied using the DBSCAN algorithm (density-based spatial clustering of applications with noise), which is efficient and robust against noise. For each material type, spatial clusters containing at least 50 pixels were used to calculate an average spectrum. This average spectrum per object was then further analyzed through principal component analysis (PCA) to facilitate the distinction between rigid and film plastics. The DBSCAN algorithm is used in preprocessing, where it finds spatial clusters of the same material in an image. These clusters yield a more reliable average spectrum for identifying whether an object is more likely to be a film or a rigid object. A limit to this clustering algorithm is that overlapping objects of the same material will be clustered together and further processed as one object, effectively meaning that overlapping films and rigids of the same polymer will be seen as one object and classified as either film or rigid.

2.5. Principal component analysis (PCA) for classification

To differentiate between films and rigids, a database was created with averaged spectra for both rigid and film PE and PP plastics, separated by hand from DKR-350 and DKR-310 waste streams and containing various contamination levels. PET film was excluded from PCA due to its limited occurrence as film packaging in Dutch post-consumer waste streams. PCA was employed to reduce the dimensionality of the hyperspectral data, allowing for effective visualization and differentiation between rigid and flexible plastics based on their average reflectance spectra. As illustrated in Figure 5, the PCA plot clearly separates rigid and flexible PE, demonstrating the reliability of spectral features as discriminative factors. New samples can be classified by comparing their average spectra with this PCA-based model. Cluster separation for PP materials using the first two principal components was less pronounced than for PE. Hence, a third principal component was employed for accurate classification of PP plastics, as shown in Figure S1. Datasets for these materials were obtained by manual characterization of ~50 kg source-separated DKR-350 and DKR-310 materials as stated in section 2.1. Each category was analyzed, where the average spectra per object were extracted to create a database, which was used to perform PCA.

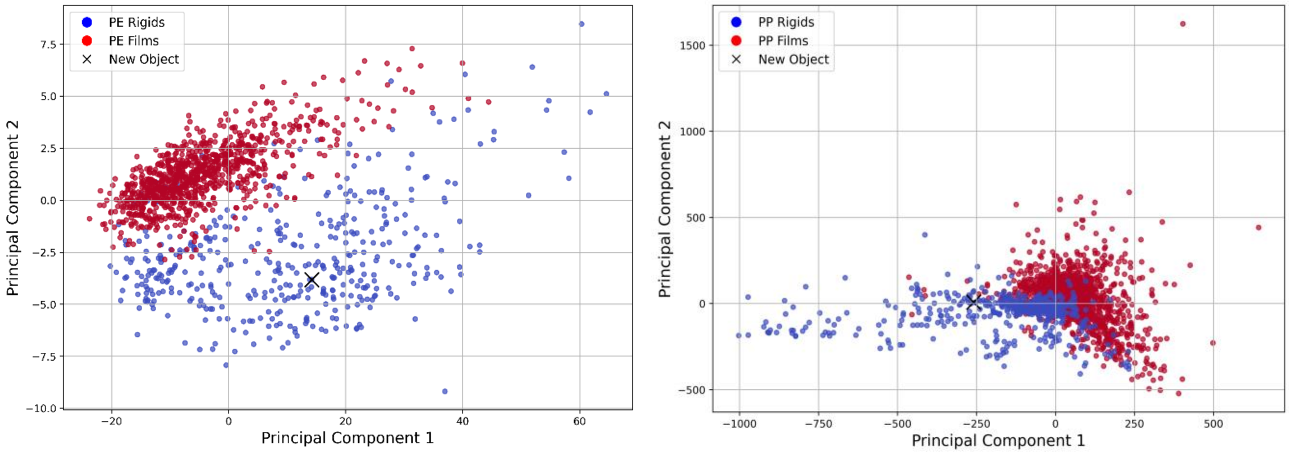

Figure 5. PCA plots for distinguishing between rigid and film plastic objects based on NIR-HSI spectral data. The left plot illustrates the clear spectral separation between PE rigids (blue) and PE films (red), while the right plot demonstrates a similar differentiation for PP rigids (blue) and PP films (red). The new object (×) is projected within the PCA space for classification based on proximity to the rigid or film clusters.

2.6. In-line analysis

For integration with existing recycling processes, we applied the model to a continuous flow of plastic waste samples (30–50 kg each of DKR-350, DKR310, and PE and PP films) on the conveyor belt at the end of the NIR optical sorter in the pilot-scale sorting line of NTCP (Figure 6). The speed of the conveyor belt in the sorting line was 2 m/s, simulating typical conveyor belt speeds in recycling facilities (e.g., for films), whereas the one with the NIR-HSI was about 1 m/s. The model predictions were compared against the actual moisture content with time measured by gravimetric analysis. Statistical tests were performed to determine the significance of differences in moisture content predictions across different plastic waste streams and moisture levels. Errors were analyzed to identify the sources of prediction errors and their impact on the overall model performance.

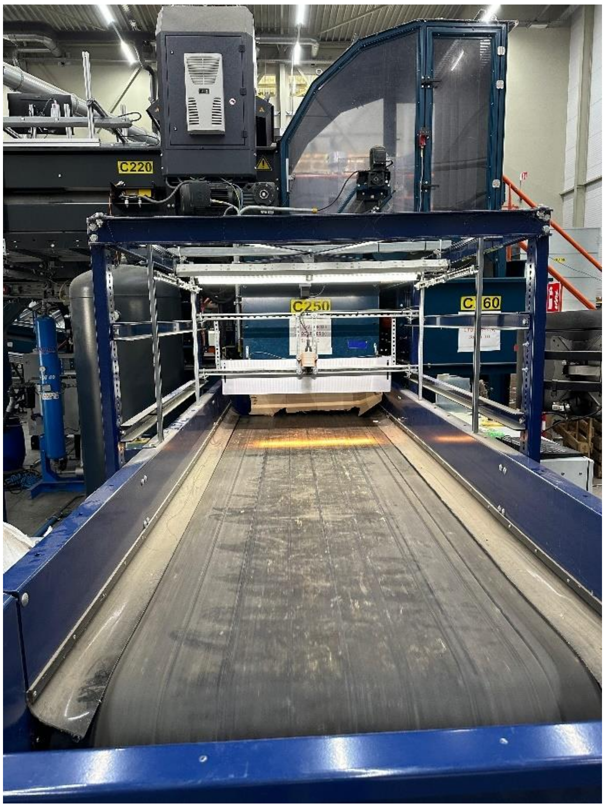

Figure 6. Photograph of the integration of the NIR-HSI imaging system for in-line moisture analysis at the end of the NIR optical sorter in the pilot-scale research sorting facility of NTCP.

3. Results and discussion

3.1. Extracting moisture absorbance

The NIR-HSI technique leverages the water absorbance peak around 1450 nm, a region in which water exhibits strong OH bond absorbance. While traditional NIR sensors provide point-based moisture measurements, NIR-HSI offers spatially resolved moisture data, which is critical for heterogeneous plastic waste. However, quantifying moisture in plastic waste presents specific challenges due to overlapping absorbance regions of water O-H bonds and plastic C-H bonds, especially in polymers like PE and PP. As shown in Figure 7, raw reflectance and absorbance spectra highlight these overlaps, with moisture absorbance partially masked by polymer-specific peaks.

To address this, an average reflectance spectrum was calculated for each polymer type, then converted to absorbance by applying a negative logarithmic transformation. The spectrum was normalized at a characteristic polymer peak around 1160 nm, where moisture absorbance is minimal. By normalizing this peak and subtracting a dry reference spectrum, we isolated the moisture signal from the polymer background. This approach allows for accurate quantification of moisture by eliminating interference from the plastic matrix, an essential step in creating a robust calibration model for various plastic types.

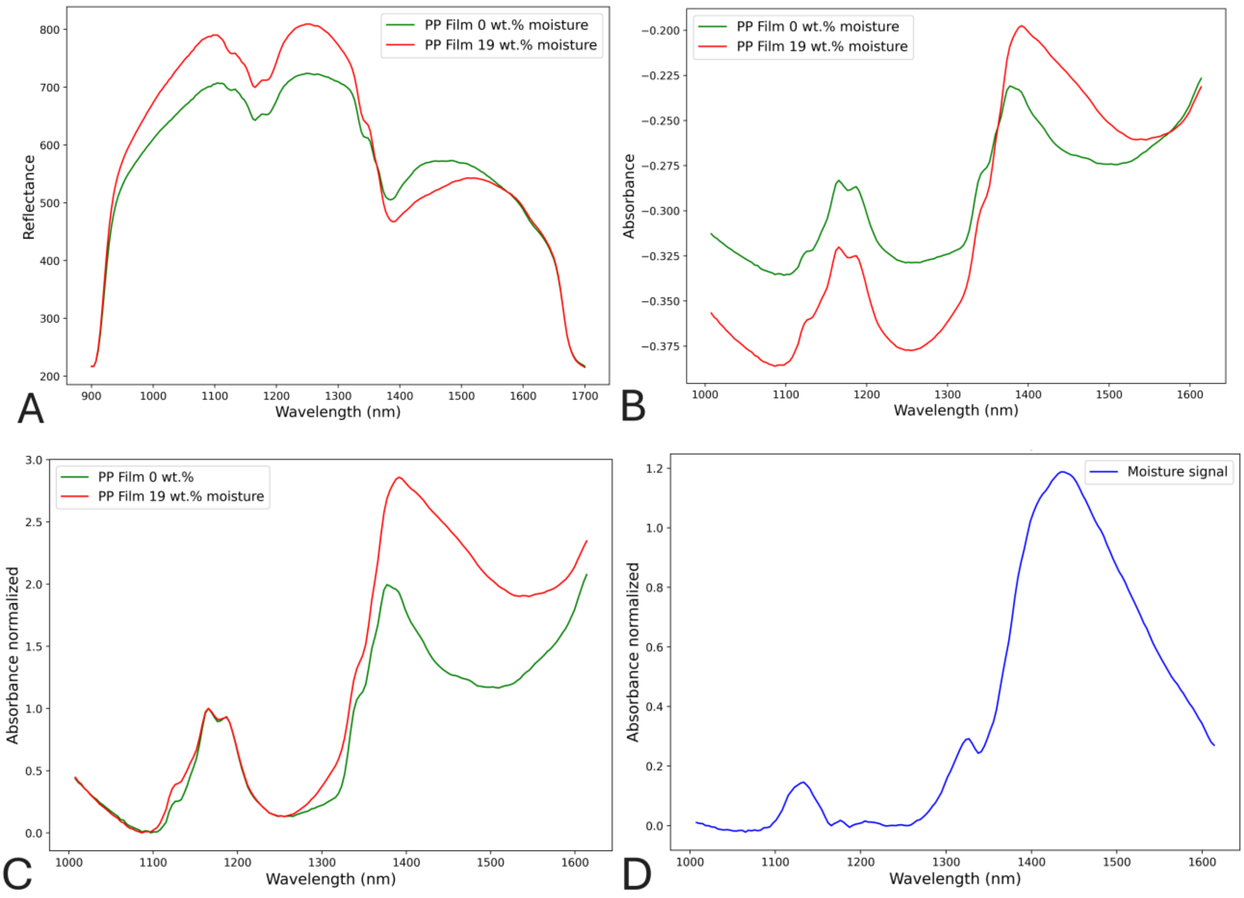

Figure 7. Example of data processing of spectra of PP film to isolate moisture absorbance: (A) raw reflectance spectra, (B) raw absorbance spectra, (C) normalized absorbance spectra, and (D) isolated moisture absorbance spectrum.

3.2. Calibration and quantification of moisture content

Isolating moisture absorbance from the spectra enabled us to employ univariate calibration for quantifying moisture content per polymer type. The integration of the moisture peak between 1400 and 1500 nm—chosen to accommodate temperature-dependent shifts in O-H absorbance—was directly correlated with gravimetrically determined moisture concentrations. As seen in Figure 8, the area under this peak differed between plastic types, providing a basis for material-specific calibration.

Calibration curves for PE and PP films, PE and PP rigids, and PET were established by correlating the integrated peak intensity (from Figure 8) with gravimetric moisture content (Figure 9). The high R^2 values across the materials underscore the precision of the model, indicating strong linearity in moisture response. Notably, differences in slope between material types highlight the unique interaction each plastic type has with NIR light, necessitating tailored calibration models for rigids and films.

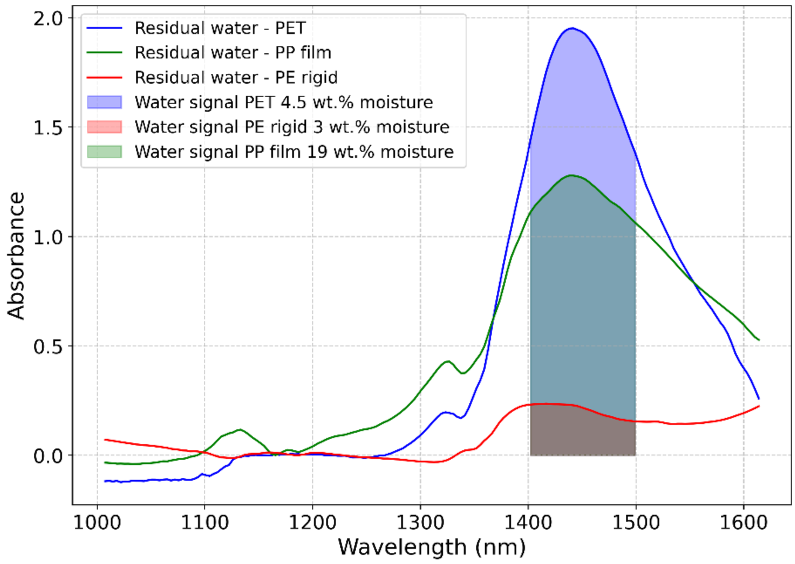

Figure 8. Spectral comparison of residual water absorbance in PE rigid (red line), PP film (green line), and PET (blue line). Shaded regions indicate the primary water absorbance bands for each plastic type (PE rigid in brown, PP film in green, and PET in violet).

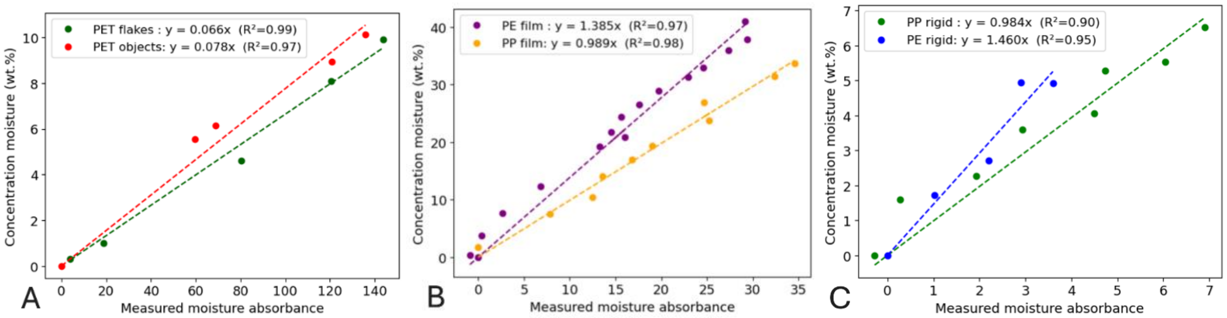

Figure 9. Calibration curves for moisture quantification in different plastic types and forms. Each panel displays the relationship between measured moisture absorbance and gravimetrically determined moisture concentration (wt%) for specific plastic categories, showing high linearity: (A) PET flakes and objects, (B) PE and PP films, and (C) PE and PP rigids.

3.3. Composition estimation and moisture quantification in mixed plastic waste samples

In addition to pixel composition analysis, we computed mass-based moisture concentrations by applying pixel-to-mass conversion factors for each plastic type. Rigid plastics, which produce fewer pixels per unit mass than films, required higher scaling factors to accurately represent their mass-based contributions. For instance, PP rigids showed a substantial difference between pixel-based and mass-based composition (7.6% vs. 24.5%), highlighting the importance of accurate scaling. Conversely, PE and PP films have lower mass composition compared to their pixel compositions, indicating they are lighter per unit area.

Using these factors, the overall mass composition of each pixel was calculated, enabling a more accurate estimation of moisture content in mixed samples (see Figure S2 and Table S2 in the Supplementary Information). This pixel-to-mass adjustment is critical for industrial applications, where mixed waste streams need accurate, rapid moisture quantification to optimize drying and recycling efficiency.

3.4. Model validation and accuracy assessment

An experiment was conducted using 10 plastic waste samples taken from a stream of DKR-350 mixed plastics. The average composition of these samples, determined manually, is shown in Figure 10 (see also Table S2 in the Supplementary Information). The major components of this stream are PE film, PP film, and PET tray, with PE film being the most dominant at 40 wt%. Other significant components include PP rigid, PET bottle, and multilayer materials. Some categories, such as metals, paper, cardboard, and textiles, are either very minor or not present in the samples. Results show that approximately 86% of the material is measurable with the developed NIR-HSI method, meaning that it falls under the categories of PE, PP, and PET. The composition of each sample, once characterized by NIR-HSI, was compared to the manually measured composition. The discrepancy between these compositions was calculated by dividing the real composition by the pixel composition. This process was repeated for all samples, and the average factor per category was calculated. The average factors are influenced by various material properties. Materials that are difficult to detect and have a low surface area to mass ratio generate fewer pixels, resulting in a higher factor to compensate for the underrepresented material.

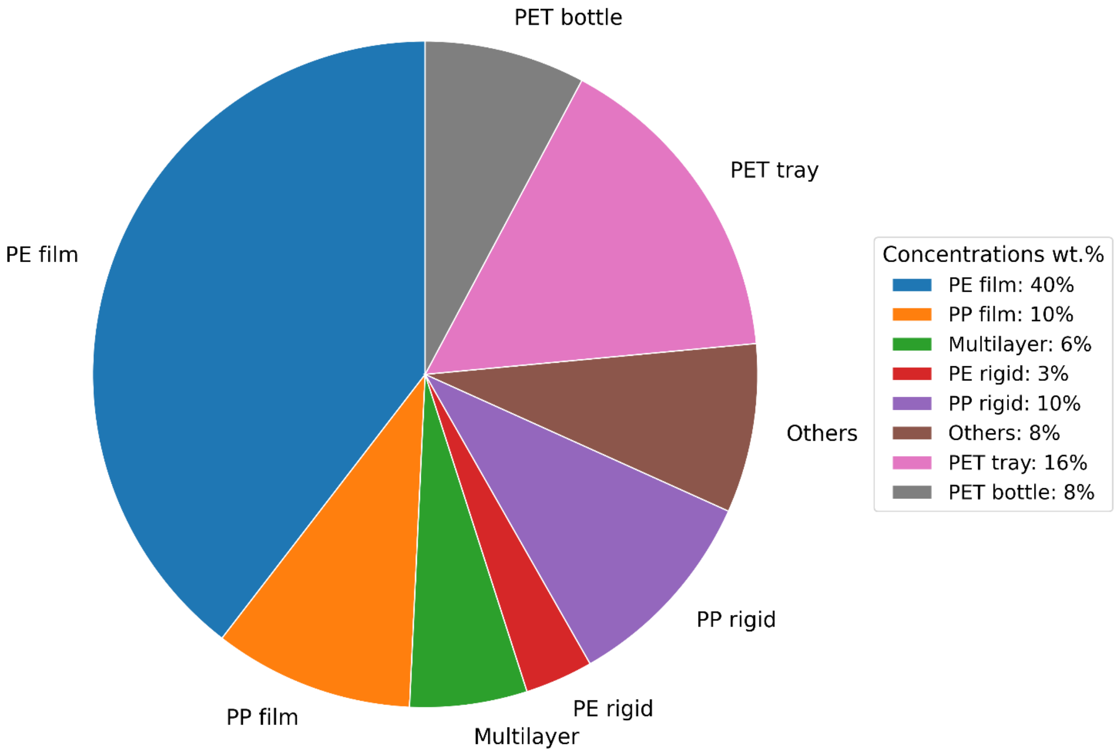

Figure 10. Average material composition (wt%) of 10 plastic waste samples of DKR-350 mixed plastics determined by manual characterization.

The model was subsequently implemented into a practical automated analysis system. The accuracy of the model was further evaluated by analyzing a diverse range of samples. All samples were recorded using the NIR-HSI camera and subsequently analyzed using the standard gravimetric method. The results obtained from both methods were compared with the gravimetric method serving as the reference standard. Samples used for validation were gathered from source-separated DKR-350 on a different date from the samples used for model development. As outlined in section 2.1, for each category, materials were separated and analyzed with NIR-HSI as well as the gravimetric method. Figure 11 shows the parity plot visualizing the accuracy of the model that predicts the moisture concentration from the true concentration, along with a confidence interval at 95% (shaded area). The margin of error is calculated to be 2.6 percentage points for 95% of the cases, indicating that the model generally performs well, with some variation in accuracy across different materials. Specific materials like PE film (shown as yellow stars) show a tendency toward under-prediction, whereas PE and PP rigids generally demonstrate high accuracy.

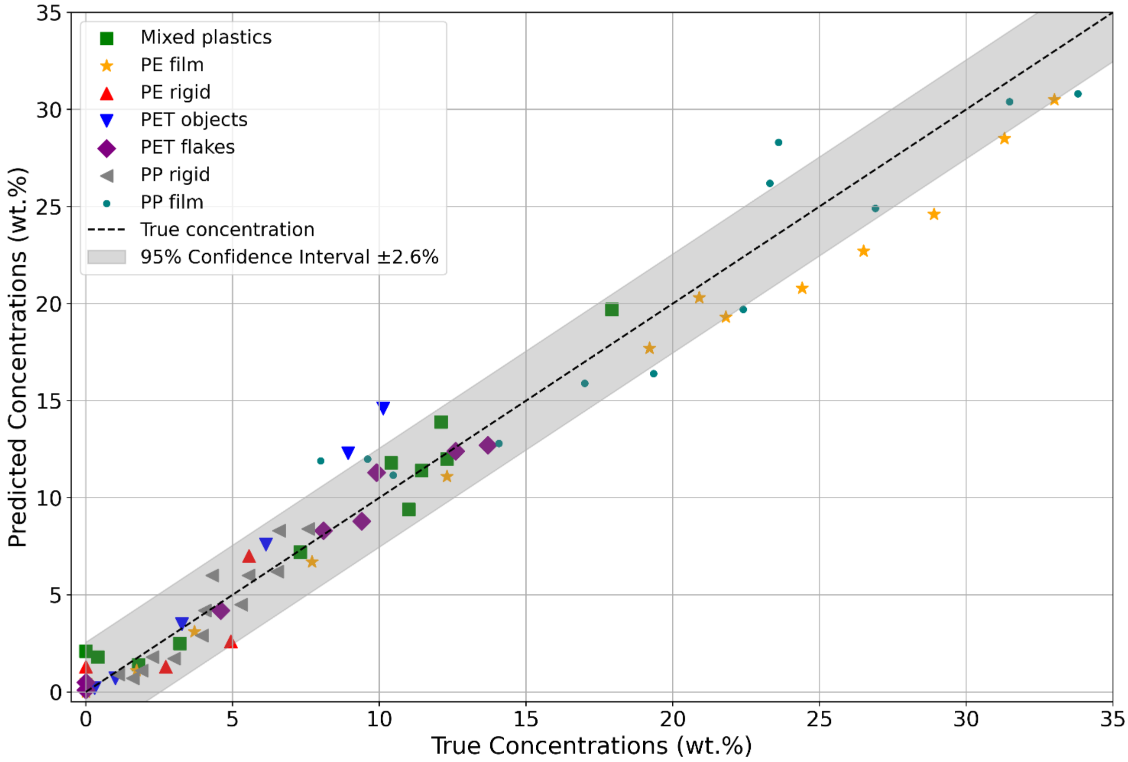

Figure 11. Parity plot comparing predicted moisture content with true moisture concentrations across different plastic types under study. The dashed line represents the line of perfect agreement (true concentration), and the shaded area indicates the 95% confidence interval.

There are several probable reasons why the predicted moisture contents of PE and PP films are generally less accurate than those of their rigid counterparts. Within a single film, thickness is typically uniform; however, small variations can affect NIR light penetration and reflectance, introducing inconsistencies in moisture predictions. Across different films, thickness uniformity is not always comparable, which can vary significantly between batches and types of films. This variation can complicate the development of a single, reliable calibration model for all films. Schwanninger et al. highlighted that thickness variations in films (10%) can cause a 5%–10% error in moisture content prediction due to inconsistent light absorption [23]. The thinner nature of films leads to a lower signal-to-noise ratio in NIR, making moisture predictions less reliable. Moreover, films often have smoother surfaces compared to rigid plastics, which can lead to high reflectivity and less consistent NIR light absorption. The research by Workman and Weyer [24] indicated that smooth surfaces can exhibit higher reflectance variability, impacting moisture readings. This can lead to lower apparent moisture content as less NIR light is absorbed by the moisture within the film. Finally, transparency, common in plastic films, exacerbates these issues, as transmitted NIR can pass through the film with little to no interaction, resulting in unwanted absorption by the conveyor belt beneath the samples rather than by the moisture within the films.

In rigid plastics, the bulkier structure allows NIR light to interact more with the moisture content distributed throughout the material. This bulk sensitivity provides a stronger moisture signal for NIR-HSI, leading to more accurate moisture content readings. Thus, the interaction of NIR light with plastic materials is heavily influenced by the physical characteristics of plastic waste samples. NIR-HSI may be more sensitive to the bulk properties of thicker materials, which can result in higher moisture readings for rigid plastics. For films, the technique might not pick up as much moisture content due to their lower thickness and different interaction with NIR light.

Moreover, the accuracy of the developed model can be compromised by limitations related to object detectability. As outlined in section 2.2, black plastics often exhibit low reflectance and are frequently undetectable by NIR systems. This lack of detectability leads to an inability to measure surface moisture accurately, causing systematic underestimations in actual moisture content. A similar limitation arises for materials not identified as PE, PP, or PET, or those heavily contaminated. Without proper material classification, extracting a clear water spectral signal from the polymer background becomes unfeasible, thereby impeding accurate moisture quantification. Although calibration was designed to mitigate such issues by encompassing a broad and heterogeneous range of samples, these detectability-related challenges inevitably introduce some degree of measurement uncertainty.

3.5. Spatial mapping and visualization of moisture distribution

Gravimetric methods cannot distinguish whether moisture tends to be more evenly distributed throughout the material or concentrated near the surface. Using the developed NIR-HSI method, we detected and quantified the precise location of moisture within various materials, a feature that is not always available or emphasized in other reported NIR-HSI techniques [27]. This could be beneficial in enhancing quality control and process optimization, providing a more predictable impact on subsequent recycling processes such as shredding and drying. The method involved analyzing a series of real plastic waste samples with varying moisture contents. As depicted in Figure 12, NIR-HSI effectively identified regions of moisture within the samples, with a clear distinction between dry areas (as indicated in yellow) and moist areas (as indicated in blue) using color gradients for easy identification. This surface localization leads to an overall moisture content detectable by NIR-HSI. For example, Figure 12A shows the difference in moisture concentrations between the PE bottle and the PE foam, with the latter containing significantly higher moisture (9.2% overall moisture) and appearing to be more concentrated near the surface, which could potentially influence drying dynamics. In another example, Figure 12B shows high moisture concentration inside the PE film (left) and the distributed moisture throughout the material (right) (22.4% overall moisture). Overall, these maps could assist in studying the properties of real plastic waste and how moisture content (even small pockets of moisture) affects its behavior and characteristics.

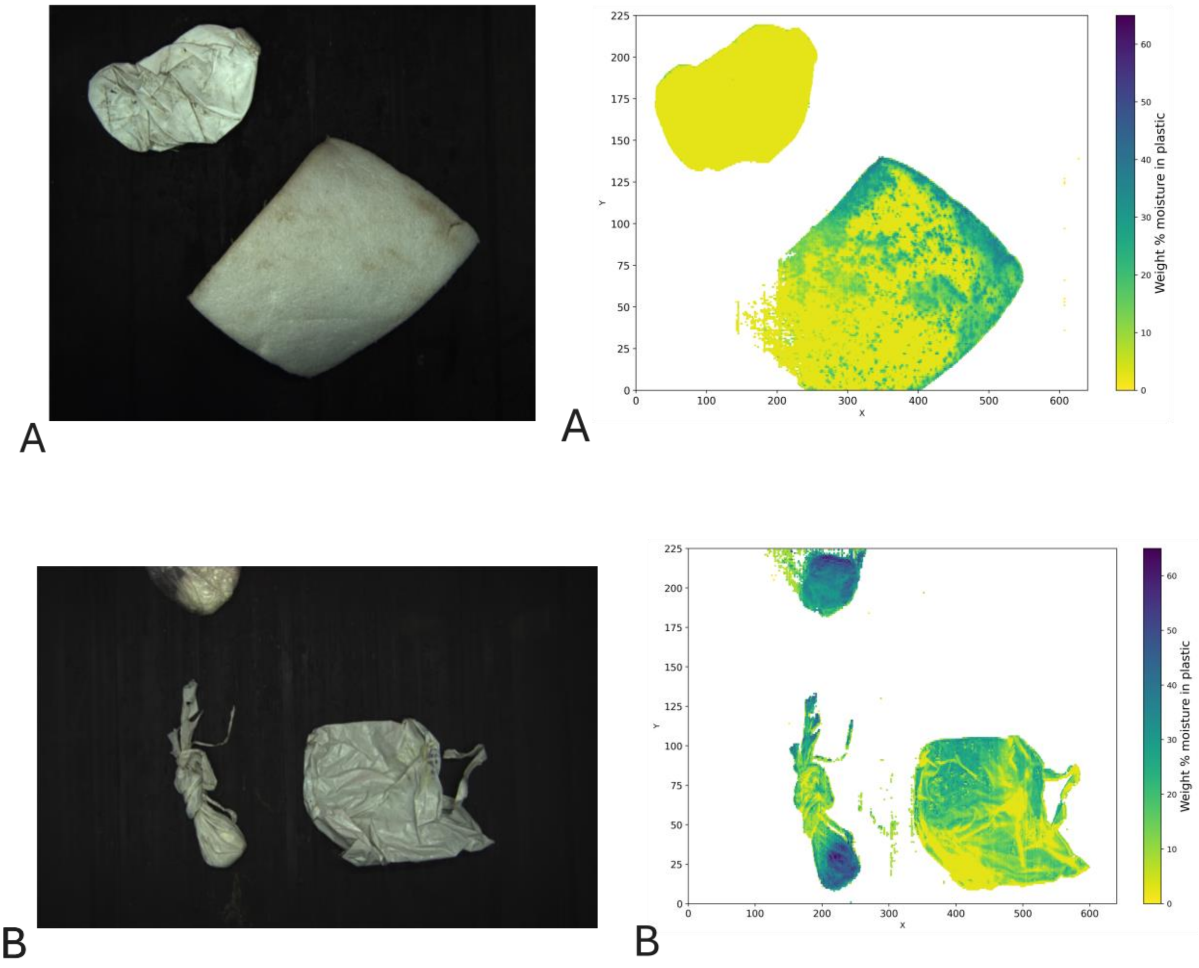

Figure 12. Visualization of moisture distribution in plastic waste samples using NIR-HSI: (A) PE rigids and (B) PE films. Also shown are the RGB images (left) and the corresponding moisture distribution maps (right).

3.6. In-line application in a pilot-scale sorting facility

The application of the model for real-time monitoring on a continuous flow of real plastic waste samples in an actual sorting facility can demonstrate its practical utility. By measuring moisture in a sorting facility, more representative and rapid measurements of moisture levels can potentially be achieved. This present study thus set up the method in a pilot-scale research sorting line at NTCP to test the monitoring of moisture levels in large batches, each exceeding 30 kg. During the trials, small waste samples (~1–2 kg) were collected and analyzed using the gravimetric method to validate the results from these in-line measurements.

Figure 13 shows a time series chart showing the moisture concentration of DKR-350 mixed plastic waste, with an overlay of volume data as a bar chart. Additionally, detailed breakdowns of specific time points with moisture concentration values using the gravimetric method are included. Moisture concentration shows significant variability over the observed period, with several peaks indicating higher moisture concentrations. These fluctuations are due to changes in moisture in the plastic material being processed. The volume data provides context for the moisture concentration fluctuations, indicating that changes in the amount of plastic waste material can significantly impact moisture concentration measurements. The weighted average moisture concentration lines provide a useful baseline to understand overall trends and deviations in the data measurements. For DKR-350, for example, the calculated weighted average concentration is 10.2% with a ±2.5% error at 95% confidence. This accuracy is deemed sufficient for practical applications in recycling, where precise moisture content determination is crucial for optimizing sorting and processing efficiency. The gravimetric measurements revealed significant variability within streams, indicating that a single-point sample is indeed not representative of the entire 50 kg batch. This in-line analysis, therefore, provides a more comprehensive view of actual moisture content and distribution within the waste batch using actual plastic waste samples.

The model performance was consistent across various sample types, including PE films and rigids, PP films and rigids, PET, and DKR-310 films/foils (see Figures S3–S8 in the Supplementary Information). Although slight variations in spectral response were observed for PP films due to inherent material properties, the model successfully adjusted for these differences. Key sources of prediction error included transparency, sample thickness, and, to some extent, environmental conditions. Changes in ambient conditions, such as lighting, temperature, and humidity during imaging, might have introduced some noise, highlighting the need for controlled imaging environments, especially when this method is applied in industrial applications. Thus, implementing controlled lighting and environmental conditions can minimize external noise and enhance data quality.

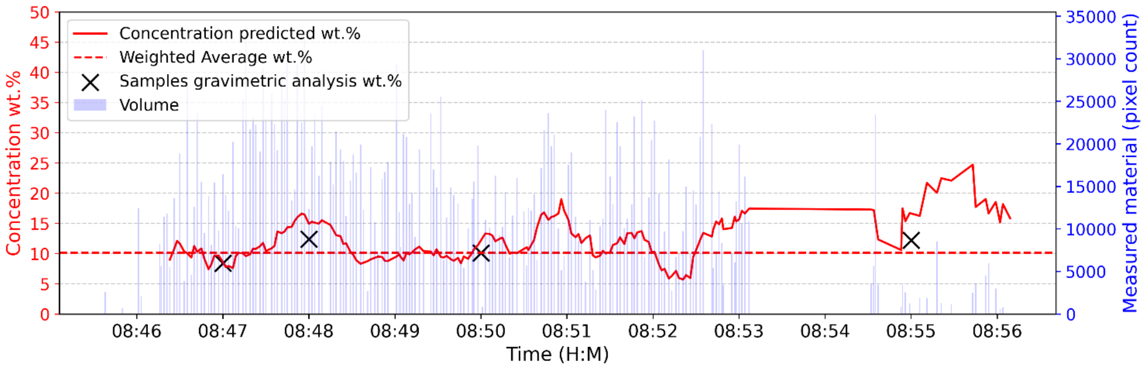

Figure 13. Time series of predicted moisture concentration in DKR-350 mixed plastic waste (~50 kg) compared with gravimetric analysis and material volume data. The red line represents the predicted moisture concentration (wt%) over time, the dashed line indicates the weighted average moisture concentration, and the × mark shows the moisture content measured by gravimetric analysis for selected samples, serving as reference points.

4. Conclusions

This study demonstrates the potential of the developed NIR-HSI method as a robust analytical tool for quantifying moisture content in real household plastic waste streams, including PE and PP films and rigids, as well as PET. Validated with 69 plastic waste samples, the model achieved a high prediction accuracy with a maximum deviation of 2.6 percentage points at a 95% confidence level, underscoring its reliability for industrial applications. Several factors were identified that collectively contribute to the higher predicted moisture content in films as compared to rigid plastics, likely due to differences in surface area, density, and structural properties affecting moisture retention. Notably, the NIR-HSI method not only accurately estimated overall surface moisture but also successfully mapped local moisture variations within individual plastic types, providing a detailed moisture profile that enhances quality control capabilities. The successful implementation of the NIR-HSI model in an actual sorting research facility demonstrates its potential for in-line quality control, allowing facilities to monitor and regulate moisture levels to ensure that plastic waste meets specified moisture content requirements. Accurate moisture quantification is essential for optimizing sorting processes and determining the most efficient handling methods for different types of waste streams, as moisture content directly influences, for example, processing efficiency, energy consumption, and the composition of recycled output.

Future research should aim to develop models tailored for industrial-level applications, addressing the challenges identified in this present study. Extensive field trials in commercial recycling facilities are needed to validate the model under diverse operational conditions. Such trials will assess the robustness and scalability of the NIR-HSI system, ensuring it can handle large volumes and diverse plastic waste streams with varying contamination levels. Using NIR-HSI for moisture measurements at the pre- and post-baling stages could yield valuable insights into the moisture content of plastic waste bales, directly impacting their market value, handling requirements, and storage conditions. Future research should also explore extending this methodology to detect and quantify other common contaminants in plastic waste, including paper and cardboard, biogenic materials, and inorganic compounds. Such advancements would make NIR-HSI a more versatile and comprehensive tool for the plastic recycling industry.

Use of AI tools declaration

The authors declare they have not used Artificial Intelligence (AI) tools in the creation of this article.

Acknowledgments

This project (“AquaSurf: Plastic waste stream characterization methods for moisture and surface contamination”) was partly financed by the TKI Chemistry (*Topconsortium voor Kennis en Innovatie Chemie*) under the PPS-allowance of the Ministry of Climate Policy and Green Growth (the Netherlands). The authors also acknowledge the support of industrial partners, namely PreZero Nederland B.V. (Harry Westerbreek and Ard-Jan Verpaalen) and Metrohm Applikon (Timoer Frelink). The authors also thank Mahdiyeh Ghaffari and Jeroen J. Jansen (Radboud University) and Tom Koopen (NTCP) for their useful discussion.

Conflict of interest

The authors declare no conflict of interest.

References

1. Plastics—the facts 2022, Plastics Europe, 2022. Available from: https://plasticseurope.org/knowledge-hub/plastics-the-facts-2022/
2. Lange JP (2021) Managing plastic waste—Sorting, recycling, disposal, and product redesign. *ACS Sustain Chem Eng* 9: 15722–15738. https://doi.org/10.1021/acssuschemeng.1c05013
3. Chen JC, Chen WH, Chang NB, et al. (2012) Interactive analysis of waste recycling and energy recovery program in a small-scale incinerator. *J Air Waste Manag Assoc* 55: 1356–1366. https://doi.org/10.1080/10473289.2005.10464723
4. Silvennoinen H (2013) The effect of moisture in certain wastes and their recovery, processing and recycling, In Bachelor's thesis, Mikkeli University of Applied Sciences. Available from: https://www.theseus.fi/bitstream/handle/10024/58614/Hanna_Silvennoinen.pdf
5. Pelayo GG, Martino AA (2023) Environmental and economic assessment of plastic waste recycling, *Publications Office of the European Union*, Luxembourg. https://dx.doi.org/10.2760/0472
6. Min K, Cuiffi JD, Mathers RT (2020) Ranking environmental degradation trends of plastic marine debris based on physical properties and molecular structure. *Nat Comm* 11: 1–11. https://doi.org/10.1038/s41467-020-14538-z
7. Elahi ADA, Bukhari S, Rehman A (2021) Plastics degradation by microbes: A sustainable approach. *J King Saud Univ Sci* 33: 101538–101550. https://doi.org/10.1016/j.jksus.2021.101538
8. Wenning HP (1993) The VEBA OEL Technologie pyrolysis process. *J Anal Appl Pyrol* 25: 301–310. https://doi.org/10.1016/0165-2370(93)80049-6
9. Delva L, Van Kets K, Kuzmanović M, et al. (2019) An introductory review: Mechanical recycling of polymers for dummies. *Plast Res*. https://www.ugent.be/ea/match/cpmt/en/research/topics/circularplastics/mechanicalrecyclingfordummiesv2.pdf
10. Hahladakis JN, Velis CA, Weber R, et al. (2018) An overview of chemical additives present in plastics: Migration, release, fate and environmental impact during their use, disposal and recycling. *J Hazard Mater* 344: 179–199. https://doi.org/10.1016/j.jhazmat.2017.10.014
11. Shan C, Pandyaswargo AH, Onoda H (2023) Environmental impact of plastic recycling in terms of energy consumption: A comparison of Japan's mechanical and chemical recycling technologies. *Energies* 16: 2199–2215. https://doi.org/10.3390/en16052199
12. Berkane I, Aracil I, Fullana A (2023) Evaluation of thermal drying for the recycling of flexible plastics. *Waste Manag* 168: 116–125. https://doi.org/10.1016/j.wasman.2023.05.054
13. Kijo-Kleczkowska A, Gnatowski A (2022) Recycling of plastic waste, with particular emphasis on thermal methods—Review. *Energies* 15: 2114–2136. https://doi.org/10.3390/en15062114
14. Gerassimidou S, Velis CA, Williams PT, et al. (2020) Characterisation and composition identification of waste-derived fuels obtained from municipal solid waste using thermogravimetry: A review. *Waste Manag. Res J Sustain Circular Economy* 38: 942–965. https://doi.org/10.1177/0734242X2094108
15. Mauer LJ, Bradley RL (2017) Moisture and total solids analysis, In *Food Analysis* Indiana (US): Purdue University West Lafayette. pp. 257–286. https://doi.org/10.1007/978-3-319-45776-5_15
16. Al-Yaari A, Dayau S, Chipeaux C, et al. (2018) The AQUI Soil moisture network for satellite microwave remote sensing validation in South-western France. *Remote sens* 10: 1839–1862.

https://doi.org/10.3390/rs10111839

17. Chen ZW, Wu J, Dou Z, et al. (2021) Design and analysis of a radio-frequency moisture sensor for grain based on the difference method, *Micromachines* 12: 708–731. https://doi.org/10.3390/mi12060708
18. Dafico LCM, Barreira E, Almeida RM, et al. (2022) Comparison of infrared thermography and other traditional techniques to assess moisture content of wall specimens. *Sensors* 22: 3182–3203. https://doi.org/10.3390/s22093182
19. Barrettino D, Badaracco G, Sala M, et al. (2023) In-line capacitive moisture sensor for polymer industries, in I2MTC, Minneapolis, MN. https://doi.org/10.1109/I2MTC.2013.6555483
20. Champagne C, McNairn H, Berg A (2011) Monitoring agricultural soil moisture extremes in Canada using passive microwave remote sensing. *Remote Sens Environ* 115: 2434–2444. https://doi.org/10.1016/j.rse.2011.04.030
21. Dafico LCM, Barriera E, Almeida MSF, et al. (2022) Comparison of infrared thermography and other traditional techniques to assess moisture content of wall specimens. *Sensors* 22: 3182–3203. https://doi.org/10.3390/s22093182
22. Tsuchikawa S, Ma T, Inagaki T (2022) Application of near-infrared spectroscopy to agriculture and forestry. *Anal Sci* 38: 635–642. https://doi.org/10.1007/s44211-022-00106-6
23. Schwanninger M, Rodrigues JC, Fackler K (2011) A review of band assignments in near infrared spectra of wood and wood components. *J Near Infrared Spectroscopy* 19: 287–308. https://doi.org/10.1255/jnirs.955
24. Workman JWL, Weyer L (2012) *Practical guide and spectral atlas for interpretive near-infrared spectroscopy*, Boca Raton: CRC Press. https://doi.org/10.1201/b11894
25. Bull C (1991) Wavelength selection for near-infrared reflectance moisture meters. *J Agr Eng Res* 49: 113–125. https://doi.org/10.1016/0021-8634(91)80032-A
26. Ciurczak EW, Igne B, Workman Jr. J, et al. (2021) *Handbook of Near-infrared Analysis*, 4 Eds., Boca Raton: CRC Press. https://doi.org/10.1201/b22513
27. Bonifazi G, D'Agostini M, Dall'Ava A, et al. (2013). A new hyperspectral imaging based device for quality control in plastic recycling, *SPIE Opt Optoelect* 8774. https://doi.org/10.1117/12.2014909
28. Manley M (2014) Near-infrared spectroscopy and hyperspectral imaging: Non-destructive analysis of biological materials. *Chem Soc Rev* 42: 8200–8214. https://doi.org/10.1039/C4CS00062E
29. Ghaffari M, Lukkien MCJ, Omidikia N, et al. (2023) Systematic reduction of hyperspectral images for high-throughput plastic characterization. *Sci Rep* 13: 21591. https://doi.org/10.1038/s41598-023-49051-y
30. Serranti S, Gargiulo A, Bonifazi G, et al. (2010) The utilization of hyperspectral imaging for impurities detection in secondary plastics. *The Open waste Manag J* 3: 56–70. https://doi.org/10.1002/(SICI)1097-4660(199709)70:1<9::AID-JCTB700>3.0.CO;2-E
31. Product specifications 04/2009. Fraction-No. 350. Mixed plastics. DKR. https://www.nedvang.nl/wp-content/uploads/2019/03/Mix-kunststoffen-DKR-350.pdf
32. Product specifications 04/2009. Fraction-No. 310. Plastic films. DKR. https://www.nedvang.nl/wp-content/uploads/2019/03/Kunststoffolie-DKR-310.pdf

AIMS Press

© 2025 the Author(s), licensee AIMS Press. This is an open access article distributed under the terms of the Creative Commons Attribution License (https://creativecommons.org/licenses/by/4.0)